

Asymmetric spreading in highly advective, disordered environments.

John H. Carpenter

Sandia National Laboratories, Albuquerque, NM 87185.

Karin A. Dahmen

*University of Illinois at Urbana-Champaign, Department of Physics, 1110 W. Green St, Urbana, IL 61801. and
Institute for Genomic Biology, 34 Animal Sciences Lab, 1207 W. Gregory Dr., Urbana, IL 61801.*

(Dated: November 15, 2018)

Spreading of bacteria in a highly advective, disordered environment is examined. Predictions of super-diffusive spreading for a simplified reaction-diffusion equation are tested. Concentration profiles display anomalous growth and super-diffusive spreading. A perturbation analysis yields a crossover time between diffusive and super-diffusive behavior. The time's dependence on the convection velocity and disorder is tested. Like the simplified equation, the full linear reaction-diffusion equation displays super-diffusive spreading perpendicular to the convection. However, for mean positive growth rates the full nonlinear reaction-diffusion equation produces symmetric spreading with a Fisher wavefront, whereas net negative growth rates cause an asymmetry, with a slower wavefront velocity perpendicular to the convection.

PACS numbers: 87.23.Cc, 87.18.-h, 05.40.-a

The study of population growth is an integral part of the biological sciences. Recently the behavior of microbial species, such as bacteria, has enjoyed much mathematical analysis due to the formation of intricate equilibrium patterns [1, 2]. Due to environmental and health concerns the behaviors in driven systems is also of interest. In this regime the dynamics are typically described using reaction-diffusion equations which may involve a number of species and their interactions [1]. While much work has been done on these types of systems, the inclusion of disorder in the environment has received limited attention. This disorder may manifest itself in a variety of ways, from spatial variations in the available food or in the presence of poisons to random diffusion constants.

In particular, a reaction diffusion equation with spatially varying growth factors may take the following form,

$$\partial_t c(\vec{x}, t) = D\nabla^2 c(\vec{x}, t) - \vec{v} \cdot \nabla c(\vec{x}, t) + [a + U(\vec{x})]c(\vec{x}, t) - bc^2(\vec{x}, t), \quad (1)$$

where the $U(\vec{x})$ are spatially random growth rates and the convection velocity v drives the population through the environment [3]. If both $U = 0$ and $v = 0$ then Eq. 1 reduces to the Fisher equation, where the growth rate a provides exponential growth which is cut off by the nonlinear interaction term b at the system's carrying capacity, a/b [1]. The linear regime of Eq. 1, around the fixed points $c = 0$ and $c = a/b$, has been studied in detail in Ref. [3]. Only some limited numerical simulation have been performed for the nonlinear case [4]. In the limit of large convection velocity v , fixed in the y direction, and with $b = 0$, a substitution of the form

$$c(\vec{x}, y, t) = \frac{1}{\sqrt{4\pi Dt}} \exp\left(at - \frac{(y - vt)^2}{4Dt}\right) W(\vec{x}, y), \quad (2)$$

allows one to obtain a simplified form of Eq. 1,

$$v\partial_t W(\vec{x}, t) = D\nabla^2 W(\vec{x}, t) + U(\vec{x}, t)W(\vec{x}, t). \quad (3)$$

Here y is relabeled as t and the directions perpendicular to y as \vec{x} [3]. As the substitution (Eq. 2) contains the exponential growth and diffusion in the y direction, the function $W(\vec{x}, t)$ describes the cross section perpendicular to the convection for a population at the 'time' $t = y/v$. Interestingly, this simplified equation has the form of an imaginary time Schrödinger equation with a random, fluctuating potential. Additionally it is directly connected to the problem of directed polymers in random media [5]. It has been shown that Eq. 3 predicts super-diffusive growth for the long time, large distance behavior, with an exponent of $2/3$ in one spatial dimension [3]. This exponent has been reproduced numerically by examining the averaged mean squared displacement of the optimal path (lowest energy path) in directed polymers [5]. Through a detailed examination of the full concentration profiles of Eq. 3, this report examines the behavior of this simplified equation in the context of population growth with the goal of obtaining a better understanding of the full equation's (Eq. 1) behavior in both the linear ($b = 0$) and nonlinear ($b > 0$) regimes. First a perturbation analysis of Eq. 3 yields a crossover time dividing pure diffusion and the super diffusive behavior. Afterwards, one dimensional numerical simulations describe concentration profiles and anomalous growth of Eq. 3 and test the predictions for the diffusion exponent and crossover time.

To obtain a perturbation expansion for Eq. 3, first note that it is an initial value problem. Thus, in the spirit of Ref. [6], one applies a Fourier-Laplace transform,

$$\widehat{W}(\vec{k}, \omega) = \int_0^\infty dt e^{-\omega t} \int_{-\infty}^\infty d^d x e^{-i\vec{k} \cdot \vec{x}} W(\vec{x}, t). \quad (4)$$

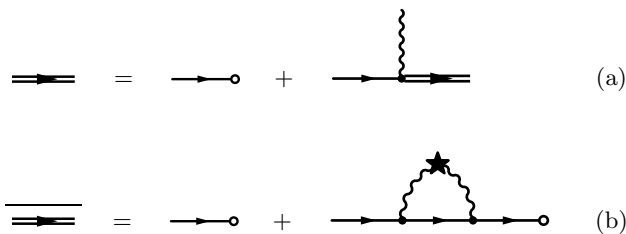


FIG. 1: Diagrammatic representation of the Fourier-Laplace transformed, simplified equation (Eq. 5). Part (a) gives the exact equation while part (b) displays the disorder averaged perturbation series to one loop order.

Equation 3 then takes the form,

$$\begin{aligned} \widehat{W}(k, \omega) &= vG_0(k, \omega)\widetilde{W}(k, 0) \\ &+ G_0(k, \omega) \int d^d q \int dt \int d\Omega_a \int d\Omega_b e^{-(\omega - (\Omega_a + \Omega_b))t} \\ &\quad \times \widehat{U}(q, \Omega_a)\widehat{W}(q, \Omega_b), \end{aligned} \quad (5)$$

with the abbreviations $\int d^d q \equiv \int_{-\infty}^{\infty} \frac{d^d q}{(2\pi)^d}$, $\int dt \equiv \int_0^{\infty} dt$, and $\int d\Omega_y \equiv \int_{y-i\infty}^{y+i\infty} \frac{d\Omega_y}{2\pi i}$ where $y = a$ or b where $G_0(k, \omega) = (v\omega + Dk^2)^{-1}$ is the free propagator and \widetilde{W} denotes taking only the Fourier transform. In obtaining this form, the Bromwich integral giving the inverse Laplace transform was used.

A graphical representation of Eq. 5 and its second order, disorder averaged expansion are shown in Fig. 1(a) and (b) respectively. As U has zero mean, upon taking the disorder average the first order term drops out. Hence determining to one loop order the renormalized propagator G_R , defined as $\widehat{W}(k, \omega) = vG_R(k, \omega)\widetilde{W}(k, 0)$, requires calculating only the second order term. For a uniform distribution of width Δ the correlator is $\overline{U(\vec{x}, t)U(\vec{x}', t')} = \frac{\Delta^2}{12} l_y^d l_t \delta^d(x - x')\delta(t - t')$ where l_y is the lattice constant for the y direction. With this fact and some straightforward contour integrations, the renormalized propagator of Fig. 1(b) becomes,

$$G_R(\vec{k}, \omega) = G_0(\vec{k}, \omega) + \frac{S_d \Delta^2 l_t}{48dv} G_0^2(k, \omega). \quad (6)$$

where S_d is the surface area of a d -dimensional sphere of unit radius. Expanding G_0 and G_R for $k \rightarrow 0$ yields

$$D_R = D \left(1 + \frac{S_d \Delta^2 l_t}{24dv^2 \omega} \right). \quad (7)$$

When the second term on the right side of Eq. 7 becomes on the order of one, then pure diffusion is no longer the dominant term. The crossover time is proportional to the value of ω^{-1} at this point. From Eq. 7 the crossover time T is given by,

$$T = \frac{48\pi dv^2}{S_d l_t \Delta^2}. \quad (8)$$

The crossover time depends on both the velocity of the flow as well as the width of the distribution of random growth rates. When the velocity increases, the system is pushed through the random environment before it has time to experience the fluctuations, seeing an effectively averaged environment. Hence it makes sense that T is increased by higher velocities. On the other hand, increasing the width of the random distribution of growth rates creates optimal paths in the system which have larger effective growth rates. This causes pure diffusion to break down earlier, hence the inverse dependence with the crossover time.

Numerical simulations of Eq. 3 were performed in one spatial dimension using a Runge-Kutta technique [7]. A Gaussian initial condition of unit variance was centered on a lattice of 20000 sites. This was large enough to insure that the boundaries were never encountered by the concentration. The random growth rates depend on time, and so must be updated during the simulation. To provide equal time and space lattice constants, a Runge-Kutta step size of 0.1 was chosen and the growth rates were updated after every ten time steps. Lastly, the concentrations were normalized after every time step.

The initial concentration profile mimics the inoculation of a medium with an initial bacterial sample. With no disorder present the Gaussian shape would persist, with a variance increasing in time. However, the disorder destroys this by providing particularly favorable paths along which growth may occur. In Fig. 2 concentration profiles are shown for two different times after inoculation. The top two plots contain profiles for a single disorder realization. For the short time there is very little deviation from the purely diffusive situation. On the other hand, the large time concentration profile deviates greatly, with large spikes developing. These regions correspond to the end of a path in the (x, t) space which had particularly favorable growth rates and thus resulted in a much larger population of bacteria than would be expected from a homogeneous environment. For the long times, these paths may end with increasing distance from the original starting position effectively shifting the mean position of the concentration from the starting position. There may also be several competing paths that have nearly the same effective growth rate resulting in several concentration spikes in the profile. These behaviors do not occur in the homogeneous case as the spreading Gaussian profile always remains centered on the starting point and symmetric about that point. Upon performing a disorder average, as seen in the bottom of Fig. 2, the large, off-center peaks result in average concentration profiles whose widths increase faster than the purely diffusive case.

The concentration profiles in Fig. 2 were normalized to have a clear comparison with the case of pure diffusion. As no growth terms are present in Eq. 3 when $U = 0$, the latter case remains normalized. This breaks down in

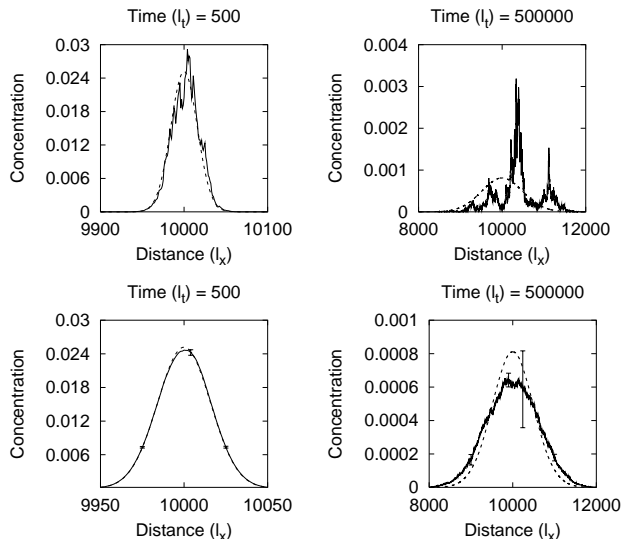


FIG. 2: Concentration profiles for one dimensional spreading according to Eq. 3, normalized by the total population. The top plots are for a single disorder realization while the bottom plots are averaged over 1000 random configurations. A Gaussian of unit variance was used as the initial profile. The solid lines are profiles for a disordered environment with $v = 4.0$ and $\Delta = 1.0$ and the dashed lines show the purely diffusive case. A maximal and several characteristic error bars are shown on the averaged distributions.

the former case however. Even though U has a zero average, fluctuations in the growth factors lead to anomalous growth. Although the effective growth is relatively small, corresponding to $a = 0.00223/l_t$ in Eq. 1 for the system shown in Fig. 2, at the longest times ($t = 500000l_t$) the effects are profound as the total population becomes on the order of e^{1100} . Clearly a diverging bacterial density is unphysical. It emerges here because the nonlinear death term has been dropped in the simplified equation, Eq. 3.

A simple argument for the appearance of this anomalous growth lies in the asymmetry between the growth and death processes. In particular, consider a small concentration of bacteria present in a favorable environment, $U > 0$. This concentration will grow exponentially in time and will spread additional concentration to neighboring areas via diffusion. On the other hand, in an unfavorable environment for growth, with $U < 0$, the local population will experience an exponential decay in concentration. While this decreases the total local population, the decrease imposed in neighboring areas is not the opposite of the growth case. The asymmetry lies in the fact that the local (and total) population cannot fall below zero. One cannot have a negative number of organisms. Hence the difference in concentration between neighboring sites, proportional to the rate of transport, is smaller with $U < 0$ leading to a reduced rate of population loss compared to the gain in population when

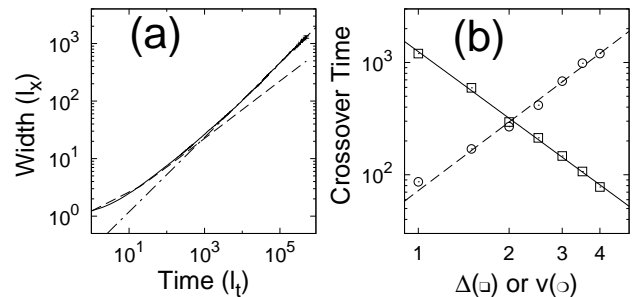


FIG. 3: Super-diffusive behaviors for the simplified equation in one dimension: (a) Concentration width vs. time averaged over 1000 disorder configurations with $v = 4.0$ and $\Delta = 4.0$ (solid line) and the purely diffusive case (dashed line). The two curves begin with a power-law of 0.5, but for long times the disordered case switches to a power-law of 0.647 ± 0.001 , shown as a dot-dash line. (b) Crossover times for variation of Δ with $v = 4.0$ (squares) and variation of v with $\Delta = 1.0$ (circles). The solid line shows a power law of -1.97 ± 0.05 and the dashed line a power law of 2.03 ± 0.10 as fit to the data varying Δ and v respectively. Each point is averaged over 3000 random configurations with statistical error bars on the order of the symbol size.

$U > 0$. Therefore the asymmetry of the diffusion process in the random environment leads to an effectively increased growth rate.

To measure the diffusion exponent, the width of the disorder averaged concentration profile, as shown in Fig. 2, was measured as a function of time. The resulting curve is shown in Fig. 3(a). For pure diffusion the profile width grows as $t^{0.5}$ as one expects. The disordered case is different, with two regions of clearly different power-law behaviors. For small times the disordered width follows the behavior of the purely diffusive case. However, as the time becomes large, the disordered case deviates from pure diffusion and instead grows with a power-law exponent equal to 0.647 ± 0.001 . This super-diffusive behavior is in good agreement with the exponent value $2/3$ that has been previously predicted [3]. As explained above, this super-diffusive behavior arises due to the appearance of optimal growth rates that deviate far from the center of the population. Upon averaging, these shift concentration from the center of the profile resulting in a width wider than the diffusive case.

A clear crossover to super-diffusive behavior is seen in Fig. 3(a). However, the location of this crossover depends on the simulation parameters. For the simulations, the predicted crossover time, Eq. 8, becomes $T = 24\pi v^2/\Delta^2$. Compared to the visually apparent crossover point in Fig. 3(a), the prediction of $T \approx 75$ is roughly an order of magnitude too small. This should not be completely unexpected as Eq. 8 really describes the time where departure from purely diffusive behavior begins. At this point the width is growing super diffusively, but does not saturate at the full exponent until $t \gg T$.

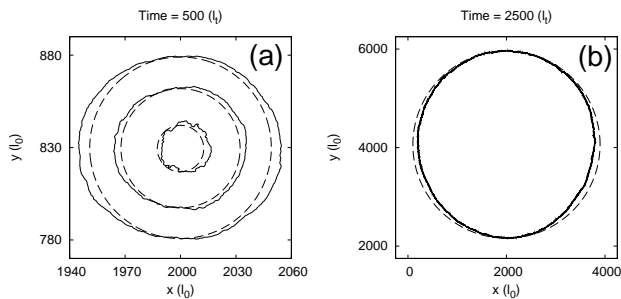


FIG. 4: Two-dimensional asymmetric spreading for the full reaction-diffusion equation (Eq. 1) with convection along the vertical axis: (a) disorder averaged concentration maps for the linear case, $b = 0$, show super-diffusive spreading perpendicular to the convection velocity for $\Delta = 2$, whereas (b), the nonlinear case $b > 0$ with $a < 0$ and $\Delta = 3$, has a wavefront that propagates more slowly in the direction perpendicular to the convection, resulting in the opposite asymmetry. For comparison, the dashed lines show the homogeneous, linear case in (a), and a circle, such as is obtained for the nonlinear case with $b > 0$ and $a > 0$, in (b).

The crossover time's dependence on the velocity and random width of the growth rates is shown in Fig. 3(b). These times were obtained at the point where the difference in width between the disordered and purely diffusive case was equal to that of a baseline case ($v = 4$ and $\Delta = 1$) at roughly the crossover time predicted by Eq. 8, $t = 1200$. The crossover times agree very well with the quadratic behavior, $T \sim (v/\Delta)^2$, predicted by Eq. 8. From Fig. 3(b) the variation with Δ at fixed v behaves as $T \sim \Delta^{-1.97 \pm 0.05}$ and the variation of v at fixed Δ results in a power-law $T \sim v^{2.03 \pm 0.10}$.

As the simplified equation describes the cross section of Eq. 1 perpendicular to the convection, it implies that Eq. 1 with $b = 0$ should exhibit super-diffusive behavior in that direction. Indeed, as seen in Fig. 4(a), the concentration contours for a two-dimensional simulation of this linear case shows contours of width equal to the homogeneous case in the direction parallel to the convection, but spreading faster perpendicular to it.

As noted above, the linear case is not physical for long times due to unrealistic organism densities. The nonlinear case with $b > 0$ presents a much different spreading picture. For $a > 0$ a symmetric Fisher wave [1] develops. This symmetry should not be completely unexpected. In the linear case, the mechanism for the enhanced spreading perpendicular to the convection was the disorder averaging of the large, asymmetric concentration spikes, such as shown in Fig. 2. Since these spikes are cut off by the carrying capacity, this behavior is absent in the nonlinear case and spreading is symmetric. The spreading is still enhanced, however, as the wavefront velocity increases with increasing disorder. In particular, outside the wavefront the linear regime applies and enhanced growth is found. Thus, one may argue [8] that the growth

rate in the Fisher velocity expression should be replaced by the real growth rate, giving the wavefront velocity

$$v_{\text{wf}} = 2\sqrt{(a_{\text{eff}}(\Delta) + a)D}. \quad (9)$$

Here a_{eff} is the effective growth rate of the corresponding linear problem which depends on the disorder strength Δ . Numerical simulations of Eq. 1 for a range of disorders find excellent agreement with this wavefront velocity [8].

The wavefront velocity expression, Eq. 9, has an important implication. Namely, attempting to poison or destroy a colony of organisms, by applying $a < 0$, may fail if the disorder creates sufficiently enhanced growth, $a_{\text{eff}} > -a$. Even more interesting, the resulting wavefront is asymmetric but in the opposite manner to the above linear case. Figure 4(b) shows the wavefront obtained from a numerical simulation of Eq. 1 with $b > 0$ but $a < 0$. The direction parallel to the convection has a wavefront velocity that follows Eq. 9, but the perpendicular wavefront velocity is smaller, resulting in an asymmetric droplet. Qualitatively, the smaller wavefront velocity arises due to the loss of optimal growth paths. The net negative growth rate does not allow paths passing regions of random, negative growth rates which were previously possible due to the additional positive growth factor. The parallel direction is unaffected, because detours around these lost paths may take place on each side of the lost paths. However, if the lost path occurs on the edge of the growing droplet, only paths nearer the droplet center remain, resulting in a reduced spreading speed.

The authors thank David Nelson and Nadav Schnerb for very useful discussions. The work was supported by NSF grant DMRs 03-25939ITR (MCC), 00-72783, and 03-14279, an A. P. Sloan fellowship (to K. D.), and an equipment award from IBM.

-
- [1] J. D. Murray, *Mathematical Biology* (Springer-Verlag, New York, 1993).
 - [2] A. J. Koch and H. Meinhardt, *Rev. Mod. Phys.* **66**, 1481 (1994).
 - [3] D. R. Nelson and N. M. Shnerb, *Phys. Rev. E* **58**, 1383 (1998).
 - [4] K. A. Dahmen, D. R. Nelson, and N. M. Shnerb, in *Statistical Mechanics of Biocomplexity*, edited by D. Reguera, J. M. G. Vilar, and J. M. Rub (Springer, Berlin, 1999), p. 124.
 - [5] T. Halpin-Healy and Y.-C. Zhang, *Phys. Rep.* **254**, 215 (1995).
 - [6] D. Forster, D. R. Nelson, and M. J. Stephen, *Phys. Rev. A* **16**, 732 (1977).
 - [7] W. H. Press, S. A. Teukolsky, W. T. Vetterling, and B. P. Flannery, *Numerical Recipes in C* (Cambridge University Press, 1992).
 - [8] J. H. Carpenter, Ph.D. thesis, University of Illinois at Urbana-Champaign (2004).